Clarifying the Supercomplex: The higher-order organization of the mitochondrial electron transport chain

James A. Letts and Leonid A. Sazanov*

Institute of Science and Technology Austria, Klosterneuburg 3400, Austria

*Correspondence: sazanov@ist.ac.at

Key words: cellular respiration, electron transport chain, supercomplexes, respirasome, membrane protein complexes, SCAF1

Abstract

The oxidative phosphorylation electron transport chain (OXPHOS-ETC) of the inner mitochondrial membrane is made up of five large protein complexes (CI, CII, CIII, CIV and CV). These complexes are responsible for converting energy from the food we eat into ATP, a small molecule that is used throughout the cell to power a multitude of essential reactions. It has been shown that the OXPHOS-ETC complexes are organized into supercomplexes (SCs) of defined stoichiometry. CI forms a supercomplex with $CIII_2$ and CIV (SC I+III_2+IV, known as the respirasome), as well as with $CIII_2$ alone (SC I+III_2). $CIII_2$ forms a supercomplex with CIV (SC III_2+IV) and CV forms dimers (CV_2). Recent electron cryo-microscopy (cryo-EM) studies have revealed the structures of SC I+III_2+IV and SC I+III_2. Furthermore, recent work has also shed light onto the assembly and function of the SCs. Here, we compare and contrast these recent studies and discuss how they have advanced our understanding of mitochondrial electron transport.

The conversion of energy from food into ATP, the universal energy "currency" of the cell, is largely carried out in the mitochondria. During cellular respiration, electrons are harvested from the metabolism of sugars, proteins and fats, and passed via the electron transport chain (ETC) to molecular oxygen (O_2). Energy from these electron transfer reactions is converted into an electro-chemical proton gradient (Δp) across the inner mitochondrial membrane by the H^+-pumping ETC complexes: NADH-ubiquinone oxidoreductase (complex I, CI), ubiquinol-cytochrome *c* oxidoreductase (complex III, CIII; also known as the cytochrome bc_1 complex) and cytochrome *c* oxidase (complex IV, CIV; **Fig 1**). Succinate-ubiquinone oxidoreductase (complex II, CII) does not pump H^+ but contributes indirectly to Δp via reduction of the ubiquinone (Q) pool (**Fig. 1**). The electrochemical energy stored in Δp is harvested by ATP synthase (complex V, CV) to synthesize ATP (**Fig 1**). The entire process is known as oxidative phosphorylation (OXPHOS) and it is among the most fundamental energy converting mechanisms for life on earth[1].

Possible higher-order organization of the OXPHOS-ETC, analogous to the "quantasome" observed in the photosynthetic chloroplast membranes of plants[2], has been debated since the 1960s[3]. The existence of an "oxysome" containing all OXPHOS-ETC complexes (CI-CV) was proposed early on[4]. However, it was later shown that each individual complex can be isolated in a functional form[5] and that mitochondrial electron transport is diffusion-coupled but not diffusion-limited[6]. These observations argued against the need for higher order structures in the OXPHOS-ETC to facilitate substrate channelling, and resulted in a random-collision model, in which all redox components are in constant and independent diffusional motion[7]. Nevertheless, the use of the gentle detergent digitonin to extract the OXPHOS-ETC complexes from the inner mitochondrial membrane revealed by Blue-Native (BN)-PAGE the existence of "supercomplexes" (SCs) of defined stoichiometry (**Fig. 2**)[8]. The majority of CI is found together with $CIII_2$ and CIV (SC I+III_2+IV), in an assembly that, together with the mobile electron carriers Q and cytochrome *c* (cyt *c*), contains all components required to pass electrons from NADH to O_2, and has been hence termed the "respirasome". This SC is distinct from the previously proposed oxysome due to its lack of CII and CV. A smaller proportion of CI is also found with $CIII_2$ alone (SC I+III_2; **Fig. 2**)[9]. Moreover, $CIII_2$ forms a SC with CIV (SC III_2+IV) independent of CI (**Fig. 2**)[8,10]. Finally, in addition to $CIII_2$, which is an obligate dimer with domain swapped Rieske iron-sulphur-protein subunits (UQCRFS)[11], CIV and CV can also form dimers (CIV_2 and CV_2; **Fig. 2**)[12-14]. Although the role of CIV_2 is unknown, formation of CV_2 is essential to membrane bending

and the formation of cristae[15]. It is important to note that the ratio of SCs varies between species and tissues[8] and may alter in response to the metabolic demands of the cell[16].

The function of the SCs has remained controversial and many initially doubted the significance of the BN-PAGE results[3,17]. Nonetheless, evidence for the SCs has mounted. It has been shown that (1) isolated respirasomes are capable of transferring electrons from NADH to O_2, i.e. they respire[18,19], (2) $CIII_2$ and CIV affect the stability of CI in the inner mitochondrial membrane[20-23], (3) SCs may reduce the amount of reactive oxygen species (ROS) produced during electron transport[24,25] and, more controversially[3,26,27], (4) SC formation may increase the transfer efficiency of the mobile electron carriers Q and cyt *c*[28], and may even trap a proportion of Q, splitting the membrane pool into two functionally distinct groups[29].

Further evidence for the existence and importance of respiratory SCs came from the discovery of specific assembly factors[29-31]. Originally, a CIV subunit homolog COX7A-RP, also known as COX7A2L and renamed SC assembly factor 1 (SCAF1), was proposed to be required for respirasome formation[29]. However, several recent studies have shown that SCAF1 is important for the stabilization of SC III_2+IV, but it is not required for assembly of the respirasome[32-34].

Definitive confirmation of respiratory SCs came recently with the elucidation of their structures at sub-nanometer resolution using cryo-EM[35-38]. The earlier structures[39,40] were at resolutions around 20 Å, which did not allow the specific interactions between the individual complexes to be resolved. The new structures, together with high-resolution structures of the individual complexes[11,12,41-44] demonstrate that the SCs form via specific interactions involving conserved residues from both the core subunits, present from bacteria to mammals, and supernumerary subunits, not generally present in bacteria, of the complexes[35,37,38].

Three different species were used for cryo-EM analyses, producing structures of bovine SCs at ~ 9 Å resolution[37], ovine at ~ 5.8 Å resolution[35] and porcine at 5.4 Å and ~4 Å resolution[36,38]. Unfortunately, the porcine structures suffer from several drawbacks. In the deposited maps (EMDB-9534 or EMDB-9539), the density for CIV is very weak (TM helices are not visible), severely limiting the reliability of its positioning and any inferred contacts. The porcine maps refined by focusing on CI or $CIII_2$ are well resolved, however, in the overall supercomplex map the contacts between CI and $CIII_2$ are not resolved at the level of the side-chains. Furthermore, most EM maps describing the intermediate states of processing are of the wrong hand (mirror image)[36,38], and in the porcine CI model (PDB 5GUP), the B-factors are not refined, the Fe-S cluster geometry and environment are incorrect, the FMN

isoalloxazine ring is flipped and model statistics were not reported, among other problems. Finally, the mechanism of electron transfer between CI and $CIII_2$ proposed[38] is inconsistent with established knowledge on $CIII_2$[45,46,47], as has also been pointed out in a recent review[48]. Thus, we will use mainly the ovine and bovine SC structures in this review, to discuss what we have learned from the structures in the context of recent work on the assembly and function of OXPHOS-ETC SCs and the implications for the role of SC formation.

Assembly and stability of the respirasome

Recent studies have shed light onto the assembly of the SCs[49,50] and the specific role of the putative assembly factor SCAF1[33,34]. It had previously been suggested that SC assembly may occur before complete assembly of the individual complexes[21]; however, a comprehensive proteomic complexome profiling study that followed nearly all CI subunits through the entire assembly process indicates, as originally proposed[18], that SC formation only occurs after complete assembly of the individual complexes[49,50]. This is likely the normal order of events, with the exception of mutant strains lacking specific subunits or assembly factors[51,52].

A controversy developed when SCAF1 was proposed to be required for the formation of SCs[29]. That proposal was based on the identification of two SCAF1 genes in different mouse lines: the full-length 113-amino acid SCAF1 in 129S2/SvPasCrlf and CD1 mice, and a short 111-amino acid form ($SCAF1^{short}$) in C57BL/6J and C57BL/6N mice[29,32]. Mitochondria from the heart and liver of mice with $SCAF1^{short}$ lacked SC III_2+IV and the respirasome, but maintained SC I+III_2, leading to the conclusion that full-length SCAF1 was required for the assembly all of SCs containing CIV[29]. These findings were in direct conflict with previous observations of SCs in heart mitochondria of C57BL/6N and C57BL/6J mice[53-55], and SCs have since been observed in liver mitochondria as well[32,56,57]. A mouse SCAF1 knockout study[31] indicated that SCAF1 was important for muscular activity and heat production and that SCAF1 supported, but was not required for, the formation of the respirasome in skeletal muscle mitochondria, with no significant effects on SC III_2+IV formation. A more detailed investigation into SC formation in the heart mitochondria of C57BL/6N and C57BL/6J mice[32] demonstrated that $SCAF1^{short}$ does not affect respirasome assembly but results in a reduction of SC III_2+IV. Taken together, these results indicated that in heart mitochondria SCAF1 is important for SC III_2+IV formation. However, SCAF1 is still found within the respirasome[29,33,56].

The first clues about the role of SCAF1 came from the structure of the respirasome[35] and knowledge of tissue-specific isoforms of CIV subunits[58-60]. In the 5.8 Å-resolution structure of the respirasome, density for the transmembrane (TM) helices of each complex was clearly visible and all density could be accounted for by the known structures of the individual isolated complexes[35]. Therefore, there was no additional density for any assembly factors, including SCAF1, which is predicted to contain a TM helix. SCAF1 is homologous to complex IV subunit COX7A, which has two tissue-specific isoforms: a heart/skeletal-muscle isoform COX7A1 and a liver-type isoform COX7A2[59]. Both isoforms are present in heart mitochondria but only COX7A2 is present in liver mitochondria, and knockout of COX7A1 is complemented by COX7A2 in the heart[61]. These observations, plus the proximity of the COX7A subunit and $CIII_2$ in the structure, led to the proposal that SCAF1 may replace the endogenous COX7A subunit to promote interactions within the respirasome[35]. Compared to COX7A1 and COX7A2, SCAF1 has an extended N-terminus that is important for interaction with $CIII_2$[33,34] and would be ideally positioned in the structure to perform this role[35].

A recent proteomics study investigating the subunit composition of SCs supports this hypothesis[33]. Respirasomes in both heart and liver mitochondria of CD1 mice were found to contain SCAF1, with a minor amount of COX7A2 found only in the heart mitochondria respirasomes[33]. The majority of the COX7A2 isoform was seen in CIV monomers[33]. In no instance was COX7A1 found in the respirasome, this isoform was almost exclusively found in CIV dimers[33]; and COX7A1 is the isoform seen in the crystal structures of CIV_2 purified from bovine heart[12,44]. Furthermore, in C57BL/6J mice containing $SCAF1^{short}$, respirasomes with either $SCAF1^{short}$ or COX7A2 were found in the heart but there was no respirasome formation in the liver[33]. In both heart and liver mitochondria, SCAF1 was also detected in SC III_2+IV and no SC III_2+IV was seen with $SCAF1^{short}$ (ref 33). These data led to the proposal that full-length SCAF1 is an assembly factor for SC III_2+IV but not required for respirasome formation in the heart (while being required in the liver)[33]. Again, this contradicts studies that found respirasome formation in the livers of mice harbouring $SCAF1^{short}$ (refs 32, 56 and 57). Nonetheless, there appears to be two separate populations of respirasomes, one containing SCAF1 and one containing COX7A2 (**Fig. 3**). This hypothesis has been bolstered by a study on respirasome assembly in heart mitochondria from both CD1 and C56BL/6J mice[34]. In this study, which focused solely on the heart, SCAF1 was found to preferentially interact with $CIII_2$ and to be essential for stabilizing SC III_2+IV but not necessary for respirasome

158 formation[34]. The authors also demonstrated that SC III_2+IV formation is not a necessary
159 precursor to respirasome formation[34].
160 Taken together, these studies suggest that there are at least two paths for the assembly
161 of the respirasome (**Fig. 3**). One path involves the early association of $CIII_2$ with SCAF1,
162 followed by the recruitment of a single copy of CIV lacking a COX7A subunit forming SC
163 III_2+IV (**Fig. 3a**). This SCAF1-containing SC then associates with CI to form the
164 respirasome (**Fig. 3a**). The second path involves early interaction between CI and $CIII_2$ in a
165 SCAF1 independent manner, followed by recruitment of a CIV monomer containing the
166 COX7A2 subunit (**Fig. 3b**). This leads to two possible populations of respirasomes[3,33]
167 differing by the presence or absence of SCAF1 or COX7A2 (**Fig. 3**)[48].
168 Given the number of different tissue-specific subunit isoforms, there is likely an even
169 more diverse population of respirasomes. The observation that the 'liver-type' COX7A2
170 isoform is incorporated into respirasomes in the heart but not the liver[33] suggests a role for
171 additional subunits or assembly factors that have yet to be identified. Since the COX7A1
172 isoform is only seen in CIV dimers it is not surprising that only COX7A2, found mainly in
173 CIV monomers, is seen in the respirasome, as according to our model only monomeric CIV
174 would be recruited into respirasomes through interaction with SC I+III_2 (**Fig. 3b**).
175 A further complication for SC characterization comes from the finding that the
176 digitonin:protein ratio used during SC extraction has a considerable effect on the amount and
177 type of SCs observed[34]. At high digitonin:protein ratios, fewer respirasomes are observed,
178 and respirasomes from mice expressing $SCAF1^{short}$ are more sensitive to the digitonin
179 concentration[34]. This suggests that, although SCAF1 is not required for the formation of the
180 respirasome, it does have a stabilizing effect when present. The digitonin sensitivity may help
181 explain the variation in observing respirasomes in liver mitochondria. In the BN-PAGE gel
182 shown in Fig. 2, the digitonin:protein ratio was 6:1 (w:w), the same as used for sample
183 preparation in the ovine structural studies[35]. For the bovine respirasome structures, a
184 digitonin:protein ratio of 28:1,or 0.11% (w/v) PCC-a-M (trans-4-(trans-4'-
185 propylcyclohexyl)cyclo-hexyl-a-D-maltoside) was used for extraction before exchange into
186 amphipols[37]. The high digitonin:protein ratio or use of PCCaM or amphipols may be
187 responsible for the higher degree of disorder and lower overall resolution of these
188 reconstructions[37]. For the porcine structures, the exact digitonin:protein ratio was not reported
189 but the SCs were extracted overnight in 1% digitonin, and given the time-dependent
190 structural changes reported for the ovine respirasome[35], these conditions may have been at
191 least partially responsible for the weak CIV density observed[36,38].

Interactions between the complexes in the respirasome

The medium-resolution structures of the respirasome, together with the high-resolution structures of the individual mitochondrial complexes, allow us to define the contacts between the complexes (**Fig. 4**)[35,41-43,62]. We describe here the main contacts between CI and $CIII_2$ and CI and CIV. Modelling of the interactions between $CIII_2$ and CIV was previously reported for the ovine structure, which contains the clearest CIV density[35]. The contacts are observed mainly between the CIV COX7A subunit and the UQCR1 and UQCR11 subunits of the adjacent CIII protomer[35].

There are two main interaction sites between CI and $CIII_2$, one in the membrane between CI subunit B14.7 (NDUFA11) and the UQCRB, UQCRQ and UQCRH subunits of the adjacent CIII protomer (**Fig. 4a**), and the other in the mitochondrial matrix between CI subunits B22 (NDUFB4) and B15 (NDUFB9) and a CIII UQCRC1 subunit (**Fig. 4b**). Notably, the interaction in the mitochondrial matrix is formed by a loop containing several negatively charged amino acid residues from the UQCRC1 subunit intercalating between the B22 and B15 subunits of CI, both containing several positively charged amino acid residues (**Fig. 4b**). All of the contacts between CI and $CIII_2$ are mediated by CI supernumerary subunits. Except for *Paracoccus dentrificans*, which contains three CI supernumerary subunits[63,64], no bacteria are known to form respiratory SCs[65]. Hence, supernumerary subunits may have evolved to facilitate the formation of SCs.

Recent experiments tracking CI assembly[50] indicated that CI is fully assembled before incorporation into SC $I+III_2$ or the respirasome and that B14.7 is added to the complex during the final assembly step. B14.7, which is essential for CI assembly and stability[49,66], dominates the interaction of CI and $CIII_2$ in the membrane (**Fig. 4a**). Therefore, CI would need to be fully assembled before stable interaction with $CIII_2$ could be established (**Fig. 4d**).

With high-resolution structures of CI now available[38,41,42], we can re-examine the interaction between CI and CIV. CI contacts the COX7C subunit of CIV via the 15th TM helix of the core antiporter-like subunit ND5 (**Fig. 4c**). In addition to possible favourable charge and polar interactions between the proteins in the mitochondrial matrix, a salt bridge likely forms between conserved residues Arg20 of COX7C and Glu503 of ND5 (**Fig. 4C**). This salt-bridge would be at the interface of the matrix and inner mitochondrial membrane, and may act to stabilize these charged groups in the hydrophobic membrane environment. It is also likely that bound lipids stabilize the interactions between the complexes. In the

structure of the porcine respirasomes[38], as in the structure of the isolated ovine CI[41], bound lipid molecules are observed. However, none of the lipids thus far identified directly bridge between the complexes. Higher-resolution structures are still needed in order to elucidate the known role of lipids in stabilizing SCs[67].

The architectures of the respirasome

Due to the ability to perform robust 3D classification of cryo-EM single particles, it is possible to identify multiple structural classes from a single data set[68]. When this was done for the ovine respirasome, two major classes were resolved, coined "tight" and "loose", that differed mainly in the position of CIV[35]. Additionally, a class of SC I+III_2 particles that lacked CIV altogether was also observed[35]. Classification of the bovine respirasomes also resulted in the isolation of three separate classes: class 1, most similar to the tight ovine respirasome; class 2, distinct from the ovine loose respirasome; and class 3, composed of SC I+III_2 particles[37].

Bovine class 1 and the ovine tight class are the most similar and populous classes and hence may represent the most stable form of the respirasome[35,37]. The bovine class 2 respirasome differs from class 1 by an ~25˚ rotation of $CIII_2$ relative to CI and CIV[37]. These structural classes demonstrate that respirasomes sample a large conformational space. Aligning by the TM domain of CI indicates that bovine and porcine CI display larger angles between the matrix and membrane arms compared to ovine. Therefore, comparison of the structures requires splitting of the respirasome into four rigid parts: the matrix arm of CI, the membrane arm of CI, $CIII_2$ and CIV. The major conformational differences can be recapitulated as rotations around a set of four pivots: a rotating hinge between the matrix and membrane arms of CI (**Fig. 5a**), a pivot at the intermembrane space side of the inner mitochondrial membrane between CI and $CIII_2$ (**Fig. 5b**), a rotation along the 2-fold symmetry axis of $CIII_2$ (**Fig. 5c**) and an internal asymmetric rotation of CIV (**Fig. 5d**). Hinge motions between the matrix and membrane arms of CI were also seen in the recent structures of isolated CI from both ovine and bovine mitochondria[41,42] and may be involved in the active to de-active transition[69,70]. A Cys residue on the TM1-TM2 loop of the ND3 core subunit of CI becomes accessible to cysteine modifying reagents in the de-active form[71] and this loop is disordered in most known structures of isolated CI[41,42], although it is observed in porcine supercomplex[38]. However, this loop is more clearly structured in a single class of bovine CI particles which differs by a rotation of the matrix arm relative to the membrane

arm[42]. Ordering and disordering of this loop likely correspond to the active/de-active transition and movement of the matrix arm may also be relevant for the turnover of the enzyme[72], but further experiments are needed. The mechanism of coupling between electron transfer in the hydrophilic arm of CI and proton translocation in the membrane arm likely involves conformational changes[41,73], but exactly how efficient coupling is achieved is still unknown and remains one of the grand challenges of bioenergetics.

Rotations about the pivot between CI and $CIII_2$ in the inner mitochondrial membrane do not appear to significantly disrupt their interactions and may be an artefact of SC extraction from the membrane (**Fig. 5b**). Conversely, the rotation of $CIII_2$ seen between bovine class 1 and class 2 likely would alter their interactions, but at the current resolution this is difficult to determine (**Fig. 5c**)[37]. In the case of movement of CIV between the ovine tight and loose respirasomes is it clear that the contacts between the complexes are altered[35]; CIV loses contact with $CIII_2$ and changes its contacts with CI. Hence, it was postulated that the loose respirasome my represent an intermediate of respirasome assembly or disassembly (**Fig. 5d**)[35]. It has been suggested that the tight and loose respirasomes may represent the SCAF1 and COX7A2 structures of the respirasome discussed above (**Fig. 3**)[33,35]. However, the resolution of these structures remains insufficient to determine the identity of the individual subunit isoforms. Additionally, the loose respirasome may be an artefact of sample preparation, as it was seen to accumulate over time after extraction from the membrane[35].

The physiological importance of the different conformational states of the respirasome observed in the extracted particles remains unknown. Some of these motions may be instrumental to enzyme turnover or dependent of specific subunit isoforms. Others are possibly artefacts of removal from the membrane. Further work is needed to distinguish between these scenarios.

Function of supercomplex formation

Stability of the individual complexes. It has been suggested that SC formation is important for the stability of the individual OXPHOS-ETC complexes[20-23]. Specifically, CIII deficiency results in a reduction of the amount of CI[20]. CI destabilization may occur via increased ROS production, since in the absence of $CIII_2$, the Q-pool becomes highly reduced[74]. However, this hypothesis does not rule out stabilization of CI by $CIII_2$ through their direct interaction in SCs. Comparison of the structures of isolated CI[35,41,42] and SCs[35-38,75] suggests how this may occur.

In the case of the isolated bovine CI, three structural classes were observed[42]. The third and smallest class had only weak density for subunit B14.7, the last half of the ND5 lateral helix and the final TM helix of ND5[42]. This bovine class 3 likely corresponds to the largest class in the ovine structure in which this region is also disordered[41]. B14.7 is the final TM subunit to associate with the complex during assembly[50] and these structures suggest that it is the first subunit lost or disordered after destabilization of CI by detergent. When compared to the other bovine classes it was shown that the angle between the core TM subunits ND2 and ND4 was larger in the absence of B14.7 (**Fig. 4e**)[42], suggesting that the lateral helix is important for the attachment of the distal pumps and revealing the important role of B14.7 in stabilizing this region (**Fig. 4e**).

A role of $CIII_2$ in stabilizing CI becomes clear in this context as the two main interaction sites between CI and $CIII_2$ bridge across the proximal and distal pumps and would further stabilize their interaction (**Fig. 4d and e**). By binding to B14.7 in the membrane and to B22 and B15 in the matrix, $CIII_2$ would prevent loss of B14.7 and hold ND2 together with the ND4 and ND5 stabilizing the entire membrane arm. Nonetheless, stabilization of CI by $CIII_2$ is unlikely the sole function of SC formation.

Reduction of ROS production. There are two main sites for ROS production in the ETC, the FMN site of CI in the matrix and the Q_P-site of $CIII_2$ in the inner mitochondrial membrane[76-79]. It has been suggested that dissociation of SC I+III_2 results in increased ROS production from CI[24], but the mechanism is unclear. Furthermore, in these studies, CI and $CIII_2$ were dissociated by addition of dodecyl maltoside (DDM) detergent near or above the critical micelle concentration[24], which is known to decrease the CI activity used to compare the total ROS produced[80] and would also disrupt the membranes.

Although generation of ROS by $CIII_2$ is thought to be small under normal conditions[78,81], inhibition of $CIII_2$ by Antimycin A considerably increases ROS production[82,83]. This is due to the Q-cycle mechanism of $CIII_2$, which takes advantage of two separate Q binding sites in each CIII protomer, Q_P and Q_N, on the positive and negative sides of the membrane, respectively. The two CIII protomers form a dimer with two separate Q-binding cavities within the hydrophobic core of the membrane; the Q_P site of one CIII protomer shares a cavity with the Q_N site of the other protomer (**Fig. 6**). Reduced QH_2 binds to the Q_P site in one cavity and transfers one electron to cyt *c* and one electron to Q bound at the Q_N site of the same monomer, releasing two H^+ into the inter membrane space (**Fig. 6**). Electron transfer to the Q_N site of the opposite monomer is possible via fast tunnelling of

electrons between the b_L haems[84], but the most likely path is within the same monomer[85] transferring the electron into the opposite Q cavity, generating an ubisemiquinone ($Q^{\bullet}$) intermediate at that Q_N site (**Fig. 6**). To finish the cycle, a second QH_2 must bind at the Q_P site and transfer a second electron to $Q^{\bullet}$, which takes up two H^+ from the mitochondrial matrix (**Fig. 6**). The other electron of the second QH_2 is used to reduce a second copy of cyt *c* and it also releases two H^+ into the inner membrane space (**Fig. 6**). This Q-cycle is the mechanism by which $CIII_2$ pumps H^+, not as a traditional H^+-pump like CI operating via an alternating access mechanism, but instead releasing H^+ into the inter-membrane space and taking up H^+ from the matrix[47,86,87]. Antimycin A binds at the Q_N sites of $CIII_2$ and prevents reduction of Q by QH_2, resulting in formation of a $Q^{\bullet}$ intermediate at the Q_P site which reacts rapidly with O_2 generating ROS[78,81,88-90]. Under normal conditions, $Q^{\bullet}$ is formed and stabilized[91] at the Q_N site[45,90,92-94], where it is shielded from O_2[95].

A possible mechanism for how ROS production may be minimized in $CIII_2$ during normal turnover revolves around symmetry breaking of $CIII_2$ by the binding of CI and CIV **(Fig. 6)**[35]. Symmetry breaking may occur by preventing the motion of the FeS UQCRFS subunit adjacent to CIV (**Fig. 6**). UQCRFS adopts two major conformations: adjacent to the Q_P site, where an electron can be transferred from reduced ubiquinol (QH_2); or adjacent to cytochrome c_1 (CYC1), where an electron can be transferred to the c_1 haem (**Fig. 6**)[96]. Movement of the UQCRFS subunit is required for electron transfer from QH_2 to cyt *c*. If the UQCRFS subunit adjacent to CIV is blocked, the Q_P site in this cavity would not be able to oxidize QH_2. Evidence for this symmetry breaking was seen in the bovine respirasome structures, in which the UQCRFS domain adjacent to CIV was ordered (indicating little conformational flexibility) and the other UQCRFS domain was disordered (indicating high conformational flexibility)[37]. This symmetry breaking would allow for the differentiation of the $CIII_2$ Q-binding cavities, in which the cavity adjacent to the CI Q-binding tunnel, the source of reduced QH_2, would be used for QH_2 oxidation, and the cavity adjacent to CIV would be used for Q reduction (**Fig. 6**). The catalytic conversion of O_2 to H_2O by CIV would ensure that the local concentration of O_2 in the vicinity is very low, making it an ideal location to shield a highly reactive intermediate (**Fig. 6**). However, as it is known that the Q_N site is not a major source of $CIII_2$ ROS, the respirasome may utilize this possible symmetry breaking for other purposes, such as ensuring efficient oxidation of QH_2 coming out of complex I. Keeping the quinol pool oxidised will allow complex I to function at the full rate

and so may help to reduce rates of ROS formation at the FMN site of complex I by driving down the NADH/NAD^+ ratio in the matrix.

Efficiency of electron transport. Recent evidence suggests that formation of SCs may be adaptive to an increased energy demand in the cell[16]. However, the question remains as to whether this is (1) to improve electron flux through the ETC, (2) to reduce the amount of ROS produced under conditions of high flux[16,25] or (3) to prevent aggregation of the complexes at higher expression levels[26,48]. Results from flux control analysis suggest that formation of SCs increase the efficiency of electron transport through substrate channelling[28] and it has even been proposed that two separate pools of Q exist: one freely diffusing in the membrane and one associated with SCs[3,27,29,97]. However, the flux control results have not been successfully replicated and showed a strong dependence on the inhibitor used[26]. Additionally, kinetic analysis in sub-mitochondrial particles (SMPs), in which the majority of the ETC complexes are in SCs, demonstrated that feeding electrons into the ETC via CI (NADH), CII (succinate) or both (NADH + succinate) did not result in significant additive effects[26]. These results are more consistent with free-exchange of Q between the membrane pool and SCs. A single pool of Q has also been demonstrated by measuring the diffusion constant of Q in the inner mitochondrial membrane[98] and the kinetics of the ubiquinone redox reactions[99,100]. Similarly, it has been shown that SC formation in *Sacchromyces cerevisiae*, which contains a SC III_2+IV_2[10,101], does not trap cyt *c*; both in the presence and absence of the SC, cyt *c* is free to diffuse in the intermembrane space[102].

The respirasome structures from bovine, porcine and ovine mitochondria clearly show that there are no protein subunits blocking free-exchange of Q with the membrane pool[35-38]. It is known that mitochondrial electron transport is a diffusion-coupled process: when the complexes are diluted in the membrane by addition of exogenous lipid, diffusion becomes rate limiting[6,103,104]. So there may be a kinetic advantage to the close proximity of the individual active sites within the SCs under conditions of high flux. Earlier work suggests that at the concentrations of all the components present in the inner mitochondrial membrane, diffusion of Q should not be rate limiting, even in maximally respiring uncoupled mitochondria[7,98]. Hence, there is no sizable kinetic advantage to be gained from substrate channelling within the respirasome and, as the structures indicate, Q should be free to exchange with the membrane pool. Whether even minor kinetic advantages due to particular orientations and accessibility of the substrate binding sites in the respirasome are useful in

mitigating ROS as described above or in ensuring maximal respiration rates remains to be established.

Future Perspectives

There is still much to learn about the structure and function of respiratory SCs. Due to their heterogeneous nature[3], the establishment of standard protocols would facilitate progress. To allow results from different studies to be easily compared, standards for the digitonin:protein ratio and extraction times should be adopted. Ideally, to reveal any trends and prevent the "cherry-picking" of ratios that maximize the difference under investigation, BN-PAGE from several digitonin:protein ratios should be presented. Additionally, in light of the influence of tissue-specific subunit isoforms[33], it is important to investigate multiple tissues to allow interpretation of results beyond the specific tissue examined.

Further structural and biochemical work on the respirasome is also needed. Structures of the respirasome in different redox states and with different bound substrates/inhibitors may help to elucidate the coupling mechanism of CI and the role of the respirasome (if any) in the regulation of the individual complexes. Furthermore, it is likely that not all factors influencing SC stability have been identified in the different tissues and additional factors should be sought out and characterized. Why is the respirasome in liver mitochondria more dependent on the presence of full-length SCAF1? Higher-resolution structures of respirasomes from different tissues may help to define structural or compositional differences. In addition, high-resolution structures of SC III_2+IV are still lacking and could reveal a great deal about the role of SCAF1 in stabilizing this complex and potentially the role of other putative SC assembly factors[105,106]. Higher-resolution structures of SC I+III_2 should also be sought, such that systematic comparisons can be made between the individual SCs and the respirasome. In the next years, we expect many of the remaining mysteries of the respirasome to be resolved, leading to a more complete picture of mammalian mitochondrial electron transport.

References

1. Nicholls, D. G. & Ferguson, S. J. *Bioenergetics 4*. (London: Academic Press, 2013).
2. Park, R. B. & Biggins, J. Quantasome: Size and Composition. *Science* **144,** 1009–1011 (1964).
3. Enríquez, J. A. Supramolecular Organization of Respiratory Complexes. *Annu. Rev. Physiol.* **78,** 533–561 (2016).
4. Chance, B., Estabrook, R. W. & Lee, C. P. Electron Transport in the Oxysome. *Science* **140,** 379–380 (1963).
5. Hatefi, Y., Haavik, A. G. & Griffiths, D. E. Studies on the electron transfer system. *J. Biol. Chem.* **237,** 1676–1680 (1962).
6. Chazotte, B. & Hackenbrock, C. R. The multicollisional, obstructed, long-range diffusional nature of mitochondrial electron transport. *J. Biol. Chem.* **263,** 14359–14367 (1988).
7. Hackenbrock, C. R., Chazotte, B. & Gupte, S. S. The random collision model and a critical assessment of diffusion and collision in mitochondrial electron transport. *J. Bioenerg. Biomembr.* **18,** 331–368 (1986).
8. Schägger, H. & Pfeiffer, K. Supercomplexes in the respiratory chains of yeast and mammalian mitochondria. *EMBO J* **19,** 1777–1783 (2000).
9. Schägger, H. & Pfeiffer, K. The ratio of oxidative phosphorylation complexes I-V in bovine heart mitochondria and the composition of respiratory chain supercomplexes. *J. Biol. Chem.* **276,** 37861–37867 (2001).
10. Cruciat, C. M., Brunner, S., Baumann, F., Neupert, W. & Stuart, R. A. The cytochrome bc1 and cytochrome c oxidase complexes associate to form a single supracomplex in yeast mitochondria. *J. Biol. Chem.* **275,** 18093–18098 (2000).
11. Iwata, S. *et al.* Complete structure of the 11-subunit bovine mitochondrial cytochrome bc_1 complex. *Science* **281,** 64–71 (1998).
12. Tsukihara, T. *et al.* The whole structure of the 13-subunit oxidized cytochrome *c* oxidase at 2.8 A. *Science* **272,** 1136–1144 (1996).
13. Davies, K. M. *et al.* Macromolecular organization of ATP synthase and complex I in whole mitochondria. *Proc. Natl. Acad. Sci. U.S.A.* **108,** 14121–14126 (2011).
14. Allegretti, M. *et al.* Horizontal membrane-intrinsic alpha-helices in the stator a-subunit of an F-type ATP synthase. *Nature* **521,** 237–240 (2015).
15. Hahn, A. *et al.* Structure of a Complete ATP Synthase Dimer Reveals the Molecular Basis of Inner Mitochondrial Membrane Morphology. *Mol. Cell* **63,** 445–456 (2016).
16. Greggio, C. *et al.* Enhanced Respiratory Chain Supercomplex Formation in Response to Exercise in Human Skeletal Muscle. *Cell Metab.* 1–12 (2016). doi:10.1016/j.cmet.2016.11.004
17. Barrientos, A. & Ugalde, C. I Function, Therefore I Am: Overcoming Skepticism about Mitochondrial Supercomplexes. *Cell Metab.* (2013).
18. Acín-Pérez, R., Fernández-Silva, P., Peleato, M. L., Pérez-Martos, A. & Enríquez, J. A. Respiratory active mitochondrial supercomplexes. *Mol. Cell* **32,** 529–539 (2008).
19. Shinzawa-Itoh, K. *et al.* Purification of Active Respiratory Supercomplex from Bovine Heart Mitochondria Enables Functional Studies. *J. Biol. Chem.* **291,** 4178–4184 (2016).
20. Acín-Pérez, R. *et al.* Respiratory complex III is required to maintain complex I in mammalian mitochondria. *Mol. Cell* **13,** 805–815 (2004).
21. Moreno-Lastres, D. *et al.* Mitochondrial complex I plays an essential role in human respirasome assembly. *Cell Metab.* **15,** 324–335 (2012).
22. Diaz, F., Fukui, H., Garcia, S. & Moraes, C. T. Cytochrome c oxidase is required for the assembly/stability of respiratory complex I in mouse fibroblasts. *Mol. Cell. Biol.*

26, 4872–4881 (2006).
23. Diaz, F., Enríquez, J. A. & Moraes, C. T. Cells lacking Rieske iron-sulfur protein have a reactive oxygen species-associated decrease in respiratory complexes I and IV. *Mol. Cell. Biol.* **32,** 415–429 (2012).
24. Maranzana, E., Barbero, G., Falasca, A. I., Lenaz, G. & Genova, M. L. Mitochondrial respiratory supercomplex association limits production of reactive oxygen species from complex I. *Antioxid. Redox Signal.* **19,** 1469–1480 (2013).
25. Lopez-Fabuel, I. *et al.* Complex I assembly into supercomplexes determines differential mitochondrial ROS production in neurons and astrocytes. *Proc Natl Acad Sci USA* (2016). doi:10.1073/pnas.1613701113
26. Blaza, J. N., Serreli, R., Jones, A. J. Y., Mohammed, K. & Hirst, J. Kinetic evidence against partitioning of the ubiquinone pool and the catalytic relevance of respiratory-chain supercomplexes. *Proc. Natl. Acad. Sci. U.S.A.* **111,** 15735–15740 (2014).
27. Lenaz, G., Tioli, G., Falasca, A. I. & Genova, M. L. Complex I function in mitochondrial supercomplexes. *BBA - Bioenergetics* **1857,** 991–1000 (2016).
28. Bianchi, C., Genova, M. L., Parenti Castelli, G. & Lenaz, G. The mitochondrial respiratory chain is partially organized in a supercomplex assembly. *J. Biol. Chem.* **279,** 36562–36569 (2004).
29. Lapuente-Brun, E. *et al.* Supercomplex assembly determines electron flux in the mitochondrial electron transport chain. *Science* **340,** 1567–1570 (2013).
30. Chen, Y.-C. *et al.* Identification of a protein mediating respiratory supercomplex stability. *Cell Metab.* **15,** 348–360 (2012).
31. Ikeda, K., Shiba, S., Horie-Inoue, K., Shimokata, K. & Inoue, S. A stabilizing factor for mitochondrial respiratory supercomplex assembly regulates energy metabolism in muscle. *Nat. Commun.* **4,** 2147 (2013).
32. Mourier, A., Matic, S., Ruzzenente, B., Larsson, N.-G. & Milenkovic, D. The respiratory chain supercomplex organization is independent of COX7a2l isoforms. *Cell Metab.* **20,** 1069–1075 (2014).
33. Cogliati, S. *et al.* Mechanism of super-assembly of respiratory complexes III and IV. *Nature* (2016). doi:10.1038/nature20157
34. Pérez-Pérez, R. *et al.* COX7A2L Is a Mitochondrial Complex III Binding Protein that Stabilizes the III_2+IV Supercomplex without Affecting Respirasome Formation. *CellReports* **16,** 2387–2398 (2016).
35. Letts, J. A., Fiedorczuk, K. & Sazanov, L. A. The architecture of respiratory supercomplexes. *Nature* **537,** 644–648 (2016).
36. Gu, J. *et al.* The architecture of the mammalian respirasome. *Nature* 1–16 (2016). doi:10.1038/nature19359
37. Sousa, J. S., Mills, D. J., Vonck, J. & Kühlbrandt, W. Functional asymmetry and electron flow in the bovine respirasome. *Elife* (2016). doi:10.7554/eLife.21290.001
38. Wu, M., Gu, J., Guo, R., Huang, Y. & Yang, M. Structure of Mammalian Respiratory Supercomplex $I_1III_2IV_1$. *Cell* **167,** 1598–1609.e10 (2016).
39. Althoff, T., Mills, D. J., Popot, J. L. & Kühlbrandt, W. Arrangement of electron transport chain components in bovine mitochondrial supercomplex $I_1III_2IV_1$. *EMBO J* **30,** 4652–4664 (2011).
40. Dudkina, N. V., Kudryashev, M., Stahlberg, H. & Boekema, E. J. Interaction of complexes I, III, and IV within the bovine respirasome by single particle cryoelectron tomography. *Proc. Natl. Acad. Sci. U.S.A.* **108,** 15196–15200 (2011).
41. Fiedorczuk, K. *et al.* Atomic structure of the entire mammalian mitochondrial complex I. *Nature* **538,** 406–410 (2016).
42. Zhu, J., Vinothkumar, K. R. & Hirst, J. Structure of mammalian respiratory complex

I. *Nature* **536,** 354–358 (2016).
43. Gao, Xiugong *et al.* Structural Basis for the Quinone Reduction in the bc1 Complex: A Comparative Analysis of Crystal Structures of Mitochondrial Cytochrome bc1 with Bound Substrate and Inhibitors at the Qi Site. *Biochemistry* **42,** 9067–9080 (2003).
44. Yano, N. *et al.* The Mg 2+-containing water cluster of mammalian cytochrome coxidase collects four pumping proton equivalents in each catalytic cycle. *J. Biol. Chem.* jbc.M115.711770 (2016). doi:10.1074/jbc.M115.711770
45. Sarewicz, M. & Osyczka, A. Electronic connection between the quinone and cytochrome C redox pools and its role in regulation of mitochondrial electron transport and redox signaling. *Physiol. Rev.* **95,** 219–243 (2015).
46. Darrouzet, E., Cooley, J. W. & Daldal, F. The Cytochrome bc1 Complex and its Homologue the b6f Complex: Similarities and Differences. *Photosyn. Res.* **79,** 25–44 (2004).
47. Mitchell, P. The protonmotive Q cycle: a general formulation. *FEBS Lett.* **59,** 137–139 (1975).
48. Milenkovic, D., Blaza, J. N., Larsson, N.-G. & Hirst, J. The Enigma of the Respiratory Chain Supercomplex. *Cell Metab.* **25,** 765–776 (2017).
49. Stroud, D. A. *et al.* Accessory subunits are integral for assembly and function of human mitochondrial complex I. *Nature* **538,** 123–126 (2016).
50. Guerrero-Castillo, S. *et al.* The Assembly Pathway of Mitochondrial Respiratory Chain Complex I. *Cell Metab.* 1–13 (2016). doi:10.1016/j.cmet.2016.09.002
51. Calvaruso, M. A. *et al.* Mitochondrial complex III stabilizes complex I in the absence of NDUFS4 to provide partial activity. *Hum. Mol. Genet.* **21,** 115–120 (2012).
52. Davoudi, M., Kotarsky, H., Hansson, E., Kallijärvi, J. & Fellman, V. COX7A2L/SCAFI and Pre-Complex III Modify Respiratory Chain Supercomplex Formation in Different Mouse Strains with a Bcs1l Mutation. *PLoS ONE* **11,** e0168774 (2016).
53. Sterky, F. H. *et al.* Altered dopamine metabolism and increased vulnerability to MPTP in mice with partial deficiency of mitochondrial complex I in dopamine neurons. *Hum. Mol. Genet.* **21,** 1078–1089 (2012).
54. Milenkovic, D. *et al.* TWINKLE is an essential mitochondrial helicase required for synthesis of nascent D-loop strands and complete mtDNA replication. *Hum. Mol. Genet.* **22,** 1983–1993 (2013).
55. Hatle, K. M. *et al.* MCJ/DnaJC15, an endogenous mitochondrial repressor of the respiratory chain that controls metabolic alterations. *Mol. Cell. Biol.* **33,** 2302–2314 (2013).
56. Williams, E. G. *et al.* Systems proteomics of liver mitochondria function. *Science* **352,** aad0189–aad0189 (2016).
57. Jha, P., Wang, X. & Auwerx, J. Analysis of Mitochondrial Respiratory Chain Supercomplexes Using Blue Native Polyacrylamide Gel Electrophoresis (BN-PAGE). *Curr Protoc Mouse Biol* **6,** 1–14 (2016).
58. Yanamura, W., Zhang, Y. Z., Takamiya, S. & Capaldi, R. A. Tissue-specific difference between heart and liver cytochrome c oxidase. *Biochemistry* **27,** 4909–4914 (1988).
59. Van Kuilenburg, A. B., Van Beeumen, J. J. & Muijsers, A. O. Subunits VIIa, b, c of human cytochrome *c* oxidase. *European Journal of …* (1992). doi:10.1111/j.1432-1033.1992.tb19847.x
60. Hüttemann, M., Kadenbach, B. & Grossman, L. I. Mammalian subunit IV isoforms of cytochrome c oxidase. *Gene* (2001).

61. Hüttemann, M. *et al.* Mice deleted for heart-type cytochrome c oxidase subunit 7a1 develop dilated cardiomyopathy. *Mitochondrion* **12,** 294–304 (2012).
62. Sun, F. *et al.* Crystal structure of mitochondrial respiratory membrane protein complex II. *Cell* **121,** 1043–1057 (2005).
63. Stroh, A. *et al.* Assembly of respiratory complexes I, III, and IV into NADH oxidase supercomplex stabilizes complex I in *Paracoccus denitrificans*. *J. Biol. Chem.* **279,** 5000–5007 (2004).
64. Yip, C.-Y., Harbour, M. E., Jayawardena, K., Fearnley, I. M. & Sazanov, L. A. Evolution of respiratory complex I: 'supernumerary' subunits are present in the alpha-proteobacterial enzyme. *J. Biol. Chem.* **286,** 5023–5033 (2011).
65. Schägger, H. Respiratory chain supercomplexes of mitochondria and bacteria. *BBA - Bioenergetics* (2002).
66. Andrews, B., Carroll, J., Ding, S., Fearnley, I. M. & Walker, J. E. Assembly factors for the membrane arm of human complex I. *Proc. Natl. Acad. Sci. U.S.A.* **110,** 18934–18939 (2013).
67. Mileykovskaya, E. & Dowhan, W. Cardiolipin-dependent formation of mitochondrial respiratory supercomplexes. *Chem. Phys. Lipids* **179,** 42–48 (2014).
68. Scheres, S. H. W. Processing of Structurally Heterogeneous Cryo-EM Data in RELION. *Meth. Enzymol.* **579,** 125–157 (2016).
69. Kotlyar, A. B. & Vinogradov, A. D. Slow active/inactive transition of the mitochondrial NADH-ubiquinone reductase. *BBA - Bioenergetics* **1019,** 151–158 (1990).
70. Vinogradov, A. D. Catalytic properties of the mitochondrial NADH-ubiquinone oxidoreductase (complex I) and the pseudo-reversible active/inactive enzyme transition. *BBA - Bioenergetics* **1364,** 169–185 (1998).
71. Babot, M. *et al.* ND3, ND1 and 39kDa subunits are more exposed in the de-active form of bovine mitochondrial complex I. *BBA - Bioenergetics* **1837,** 929–939 (2014).
72. Zickermann, V. *et al.* Mechanistic insight from the crystal structure of mitochondrial complex I. *Science* **347,** 44–49 (2015).
73. Sazanov, L. A. A giant molecular proton pump: structure and mechanism of respiratory complex I. *Nat. Rev. Mol. Cell Biol.* **16,** 375–388 (2015).
74. Guarás, A. *et al.* The CoQH2/CoQ Ratio Serves as a Sensor of Respiratory Chain Efficiency. *CellReports* **15,** 197–209 (2016).
75. Ge, J. *et al.* Architecture of the mammalian mechanosensitive Piezo1 channel. *Nature* (2015). doi:10.1038/nature15247
76. Muller, F. L., Liu, Y. & Van Remmen, H. Complex III releases superoxide to both sides of the inner mitochondrial membrane. *J. Biol. Chem.* **279,** 49064–49073 (2004).
77. Kussmaul, L. & Hirst, J. The mechanism of superoxide production by NADH:ubiquinone oxidoreductase (complex I) from bovine heart mitochondria. *Proc. Natl. Acad. Sci. U.S.A.* **103,** 7607–7612 (2006).
78. Murphy, M. P. How mitochondria produce reactive oxygen species. *Biochem. J.* **417,** 1–13 (2009).
79. Pryde, K. R. & Hirst, J. Superoxide is produced by the reduced flavin in mitochondrial complex I: a single, unified mechanism that applies during both forward and reverse electron transfer. *J. Biol. Chem.* **286,** 18056–18065 (2011).
80. Letts, J. A., Degliesposti, G., Fiedorczuk, K., Skehel, M. & Sazanov, L. A. Purification of Ovine Respiratory Complex I Results in a Highly Active and Stable Preparation. *J. Biol. Chem.* **291,** 24657–24675 (2016).
81. Forman, H. J. & Azzi, A. On the virtual existence of superoxide anions in

mitochondria: thoughts regarding its role in pathophysiology. *FASEB J.* **11,** 374–375 (1997).
82. Forman, H. J. & Kennedy, J. A. Role of superoxide radical in mitochondrial dehydrogenase reactions. *Biochem. Biophys. Res. Commun.* **60,** 1044–1050 (1974).
83. Boveris, A. & Chance, B. The mitochondrial generation of hydrogen peroxide. General properties and effect of hyperbaric oxygen. *Biochemical Journal* **134,** 707–716 (1973).
84. Swierczek, M. *et al.* An electronic bus bar lies in the core of cytochrome bc1. *Science* **329,** 451–454 (2010).
85. Crofts, A. R. *et al.* The Q-cycle reviewed: How well does a monomeric mechanism of the bc_1 complex account for the function of a dimeric complex? *BBA - Bioenergetics* **1777,** 1001–1019 (2008).
86. Mitchell, P. Protonmotive redox mechanism of the cytochrome b-c1 complex in the respiratory chain: protonmotive ubiquinone cycle. *FEBS Lett.* **56,** 1–6 (1975).
87. Osyczka, A., Moser, C. C. & Dutton, P. L. Fixing the Q cycle. *Trends in Biochemical Sciences* **30,** 176–182 (2005).
88. De Vries, S., Albracht, S. P., Berden, J. A. & Slater, E. C. A new species of bound ubisemiquinone anion in QH_2: cytochrome *c* oxidoreductase. *J. Biol. Chem.* **256,** 11996–11998 (1981).
89. Quinlan, C. L., Gerencser, A. A., Treberg, J. R. & Brand, M. D. The mechanism of superoxide production by the antimycin-inhibited mitochondrial Q-cycle. *J. Biol. Chem.* **286,** 31361–31372 (2011).
90. Ohnishi, T. & Trumpower, B. L. Differential effects of antimycin on ubisemiquinone bound in different environments in isolated succinate . cytochrome *c* reductase complex. *J. Biol. Chem.* **255,** 3278–3284 (1980).
91. Dikanov, S. A. *et al.* Hydrogen bonds between nitrogen donors and the semiquinone in the Q_i-site of the bc_1 complex. *J. Biol. Chem.* **282,** 25831–25841 (2007).
92. Yu, C. A., Nagaoka, S., Yu, L. & King, T. E. Evidence for the existence of a ubiquinone protein and its radical in the cytochromes b and c1 region in the mitochondrial electron transport chain. *Biochem. Biophys. Res. Commun.* **82,** 1070–1078 (1978).
93. Yu, C. A., Nagoaka, S., Yu, L. & King, T. E. Evidence of ubisemiquinone radicals in electron transfer at the cytochromes *b* and c_1 region of the cardiac respiratory chain. *Arch. Biochem. Biophys.* **204,** 59–70 (1980).
94. De Vries, S., Berden, J. A. & Slater, E. C. Properties of a semiquinone anion located in the QH_2:cytochrome *c* oxidoreductase segment of the mitochondrial respiratory chain. *FEBS Lett.* **122,** 143–148 (1980).
95. Raha, S., McEachern, G. E., Myint, A. T. & Robinson, B. H. Superoxides from mitochondrial complex III: the role of manganese superoxide dismutase. *Free Radic. Biol. Med.* **29,** 170–180 (2000).
96. Xia, D. *et al.* Structural analysis of cytochrome bc_1 complexes: implications to the mechanism of function. *BBA - Bioenergetics* **1827,** 1278–1294 (2013).
97. Genova, M. L. & Lenaz, G. Functional role of mitochondrial respiratory supercomplexes. *BBA - Bioenergetics* **1837,** 427–443 (2014).
98. Gupte, S. *et al.* Relationship between lateral diffusion, collision frequency, and electron transfer of mitochondrial inner membrane oxidation-reduction components. *Proc. Natl. Acad. Sci. U.S.A.* **81,** 2606–2610 (1984).
99. Kröger, A. & Klingenberg, M. The kinetics of the redox reactions of ubiquinone related to the electron-transport activity in the respiratory chain. *Eur. J. Biochem.* **34,** 358–368 (1973).

100. Kröger, A. & Klingenberg, M. Further evidence for the pool function of ubiquinone as derived from the inhibition of the electron transport by antimycin. *Eur. J. Biochem.* **39,** 313–323 (1973).
101. Mileykovskaya, E. *et al.* Arrangement of the respiratory chain complexes in Saccharomyces cerevisiae supercomplex III_2IV_2 revealed by single particle cryo-electron microscopy. *J. Biol. Chem.* **287,** 23095–23103 (2012).
102. Trouillard, M., Meunier, B. & Rappaport, F. Questioning the functional relevance of mitochondrial supercomplexes by time-resolved analysis of the respiratory chain. *Proc. Natl. Acad. Sci. U.S.A.* **108,** E1027–34 (2011).
103. Schneider, H., Lemasters, J. J., Höchli, M. & Hackenbrock, C. R. Fusion of liposomes with mitochondrial inner membranes. *Proc. Natl. Acad. Sci. U.S.A.* **77,** 442–446 (1980).
104. Schneider, H., Lemasters, J. J., Höchli, M. & Hackenbrock, C. R. Liposome-mitochondrial inner membrane fusion. Lateral diffusion of integral electron transfer components. *J. Biol. Chem.* **255,** 3748–3756 (1980).
105. Strogolova, V., Furness, A., Robb-McGrath, M., Garlich, J. & Stuart, R. A. Rcf1 and Rcf2, members of the hypoxia-induced gene 1 protein family, are critical components of the mitochondrial cytochrome bc1-cytochrome c oxidase supercomplex. *Mol. Cell. Biol.* **32,** 1363–1373 (2012).
106. Vukotic, M. *et al.* Rcf1 mediates cytochrome oxidase assembly and respirasome formation, revealing heterogeneity of the enzyme complex. *Cell Metab.* **15,** 336–347 (2012).
107. Zhou, A. *et al.* Structure and conformational states of the bovine mitochondrial ATP synthase by cryo-EM. *Elife* **4,** (2015).

Figure 1. The complexes of the mitochondrial OXPHOS-ETC. The experimentally determined structural models of the mammalian mitochondrial OXPHOS-ETC complexes are shown. The atomic structures of complex I (CI, ovine, PDB 5LNK)[41], complex II (CII, porcine, PDB 1ZOY)[62], complex III (CIII, bovine, PDB 1NTM)[43], complex IV (CIV, bovine, PDB 5B1A)[44] and the medium resolution structure of complex V (CV, bovine, PDB 5ARA)[107] are shown shaded by subunit with CI dark blue-to-light blue, CII cyan-to-light green, $CIII_2$ green-to-yellow, CIV magenta-to-red and CV red-to-yellow. The atomic structure of cytochrome *c* (cyt *c*, equine, PDB 5IY5) is shown in orange. Atoms from the models are shown as spheres. The reactions catalysed by the complexes are shown. Q, ubiquinone, QH_2, ubiquinol. The approximate boundary of the membrane is indicated by the light blue rectangle with mitochondrial matrix up and intermembrane space (IMS) down.

Figure 2. The supercomplexes of the mitochondrial OXPHOS-ETC. Left, a Blue-Native (BN)-PAGE gel of digitonin extracted washed mitochondrial membranes from ovine heart. A digitonin:protein ratio of 6:1 (wt:wt) was used for the extraction. The different SCs are indicated and their approximate molecular weight and architecture are shown. Assignment of bands is based on molecular weight and comparison to proteomic and western blot studies[33,34,56]. Complexes are coloured as in Fig. 1.

Figure 3. Two possible paths for the assembly of respirasomes. Respirasome assembly may occur via a SCAF1 dependent and SCAF1 independent pathways. **a,** The SCAF1 dependent path: $CIII_2$ bound with a single copy of SCAF1 binds to CIV lacking the COX7A subunit forming SC III_2+IV followed by the addition of CI. **b,** The SCAF1 independent path: CI and $CIII_2$ come together to form SC I+III_2 which is then completed by the addition of CIV. These paths may lead to the existence of two respirasome populations differentiated by the presence of SCAF1 vs. COX7A2. It is unknown whether these different populations can exchange by swapping between SCAF1 and COX7A2. Complexes are coloured as in Fig. 1 with SCAF1 grey and COX7A orange.

Figure 4. Interaction sites within the tight respirasome. a, Interactions in the membrane between subunit B14.7 of CI and adjacent $CIII_2$ subunits UQCRB, UQCRQ and UQCRH. **b,** Interactions in the mitochondrial matrix between subunits B15 and B22 of the CI distal bulge and a UQCR1 subunit of $CIII_2$. **c,** Possible interactions between the ND5 core subunit of CI and the COX7C subunit of CIV. The insets below indicate the positions on CI of the interaction sites and the relative viewpoints in **a** and **b**. The viewpoint in **c** is not rotated from that of the inset. **d,** Surface representation of the tight respirasome viewed from the $CIII_2$ side within the membrane, $CIII_2$ and CIV are shown in green and magenta respectively and are transparent to allow visualization of the CI binding sites (shown in red). CI is shown as in the **a-c** insets with the matrix arm dark blue, the proximal (to the peripheral arm) pumps (ND1/ND3/ND6/ND4L, ND2) of the membrane arm medium blue, the distal pumps (ND4, ND5) of the membrane arm light blue and the B14.7 subunit cyan. **e,** Stabilization of CI through interaction with $CIII_2$. Schematic of CI in the tight respirasome showing the different modules of the membrane arm, B14.7 and interaction points between CI and CIII (in red). Loss of B14.7 results in disorder of part of the lateral helix and the final TM helix of ND5 (indicated by black lines) and a tilting of the distal pumps relative to the proximal pumps[41,42].

Figure 5. The four major pivots of the respirasome. Comparing the respirasome architectures from bovine and ovine mitochondria results in the identification of four major conformational pivots. **a,** Side view (mitochondrial matrix up) of the overlay of the ovine tight respirasome[35] and the bovine class 1 respirasome[37] demonstrating the tilt and rotation seen around a pivot at the interface of the matrix arm and the membrane arm. **b,** Overlay of the ovine tight and loose respirasomes[35] viewed from the "heel" of CI (mitochondrial matrix up). A pivot located at the CI, $CIII_2$ and inner mitochondrial membrane/IMS interface defines a rigid-body rotation of $CIII_2$ away from CI in the mitochondrial matrix. **c,** Overlay of the bovine class 1 and class 2 respirasomes[37] viewed from the mitochondrial matrix. A large rotation of $CIII_2$ relative to CI and CIV can be seen centred roughly along the two-fold symmetry axis of $CIII_2$. **d**, Overlay of the ovine tight and loose respirasomes[35] viewed from the mitochondrial matrix. The large motion of CIV relative to CI and $CIII_2$ about a pivot centred on CIV away from the other complexes is indicated. The complexes are shown with α-helices as cylinders and β-strands as rectangular planks coloured with CI blue, $CIII_2$ green and CIV magenta, with different shades to distinguish between the different classes. All alignments were done using the membrane arm of CI.

Figure 6. Asymmetric Electron Flow Through $CIII_2$ may reduce ROS production. Breaking the inherent symmetry of $CIII_2$ through interactions with CI and CIV may result in the formation of a CI-proximal QH_2 oxidation cavity and a CI-distal Q reduction cavity. The presence of CIV capping the Q reduction cavity may help shield the $Q^{\bullet}$ intermediate from reacting with oxygen. One possibility for symmetry breaking is steric hindrance of motion of the distal UQCRFS1 subunit (indicated by a star, FeS cluster shown in the distal position and coloured red)[35,37]. Both proximal (orange FeS cluster) and distal (red FeS cluster) are shown for the proximal UQCRFS1 indicating free-motion (double-headed arrow) of this subunit.

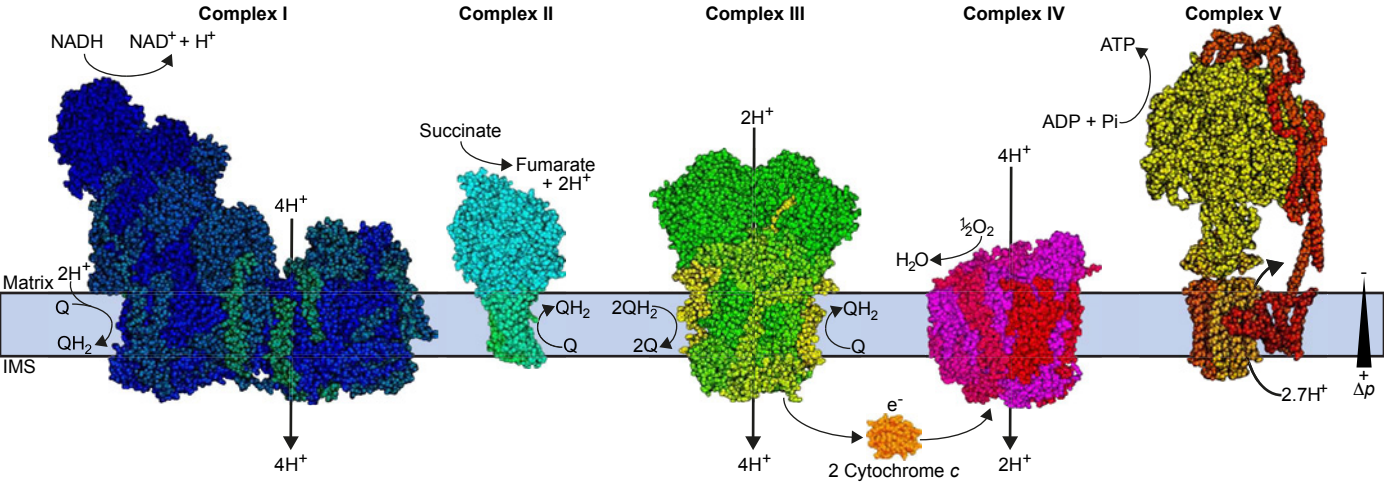
Complex I
Complex II
Complex III
Complex IV
Complex V
NADH
NAD+ + H+
4H+
2H+
Matrix
Q
QH2
IMS
4H+
Succinate
Fumarate
+ 2H+
QH2
Q
2H+
2QH2
2Q
QH2
Q
4H+
e-
2 Cytochrome c
2H+
4H+
½O2
H2O
ATP
ADP + Pi
2.7H+
-
+
Δp

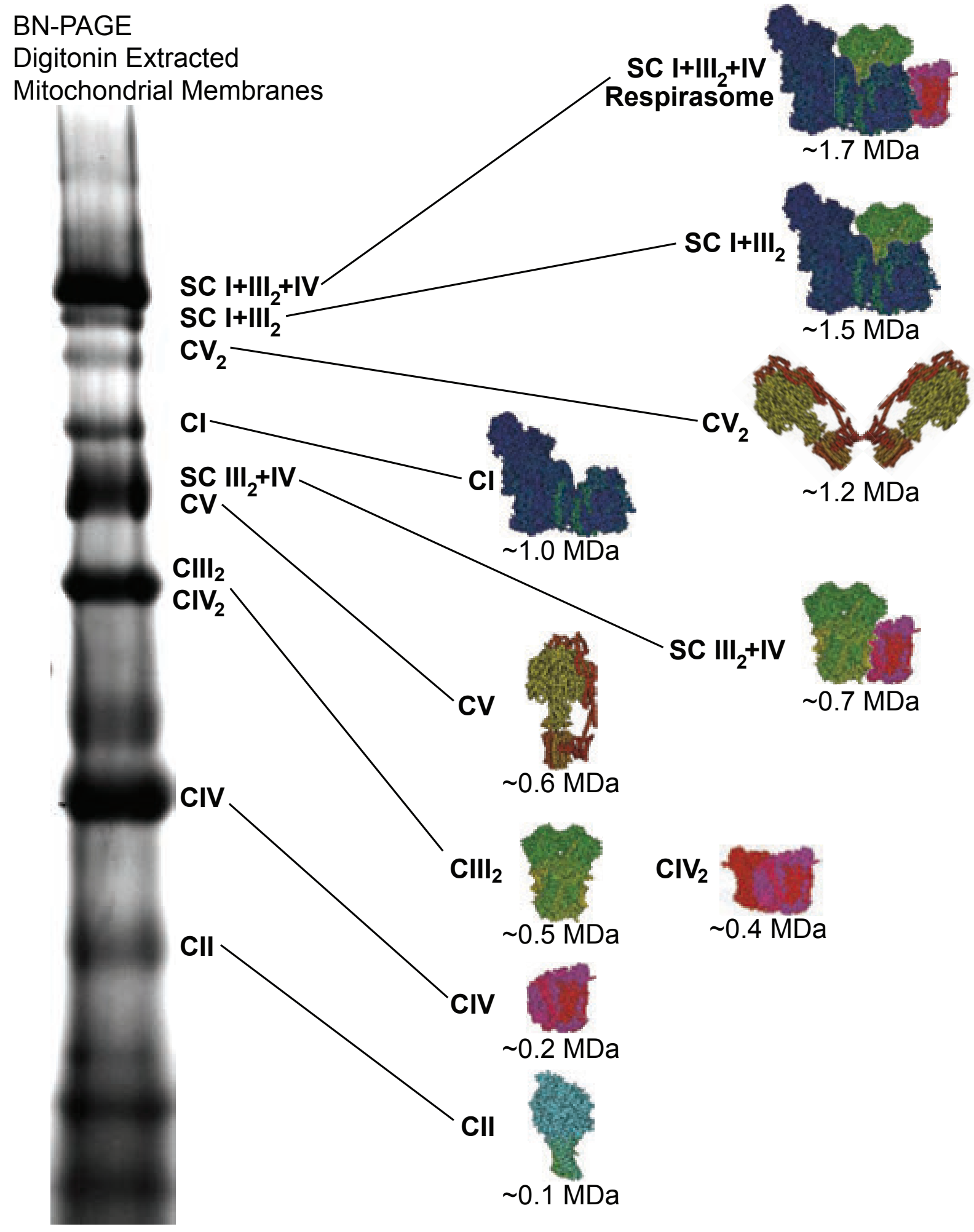
BN-PAGE
Digitonin Extracted
Mitochondrial Membranes
SC I+III2+IV
Respirasome
~1.7 MDa
SC I+III2
~1.5 MDa
SC I+III2+IV
SC I+III2
CV2
CV2
~1.2 MDa
CI
CI
~1.0 MDa
SC III2+IV
CV
CIII2
CIV2
SC III2+IV
~0.7 MDa
CV
~0.6 MDa
CIV
CIII2
~0.5 MDa
CIV2
~0.4 MDa
CII
CIV
~0.2 MDa
CII
~0.1 MDa

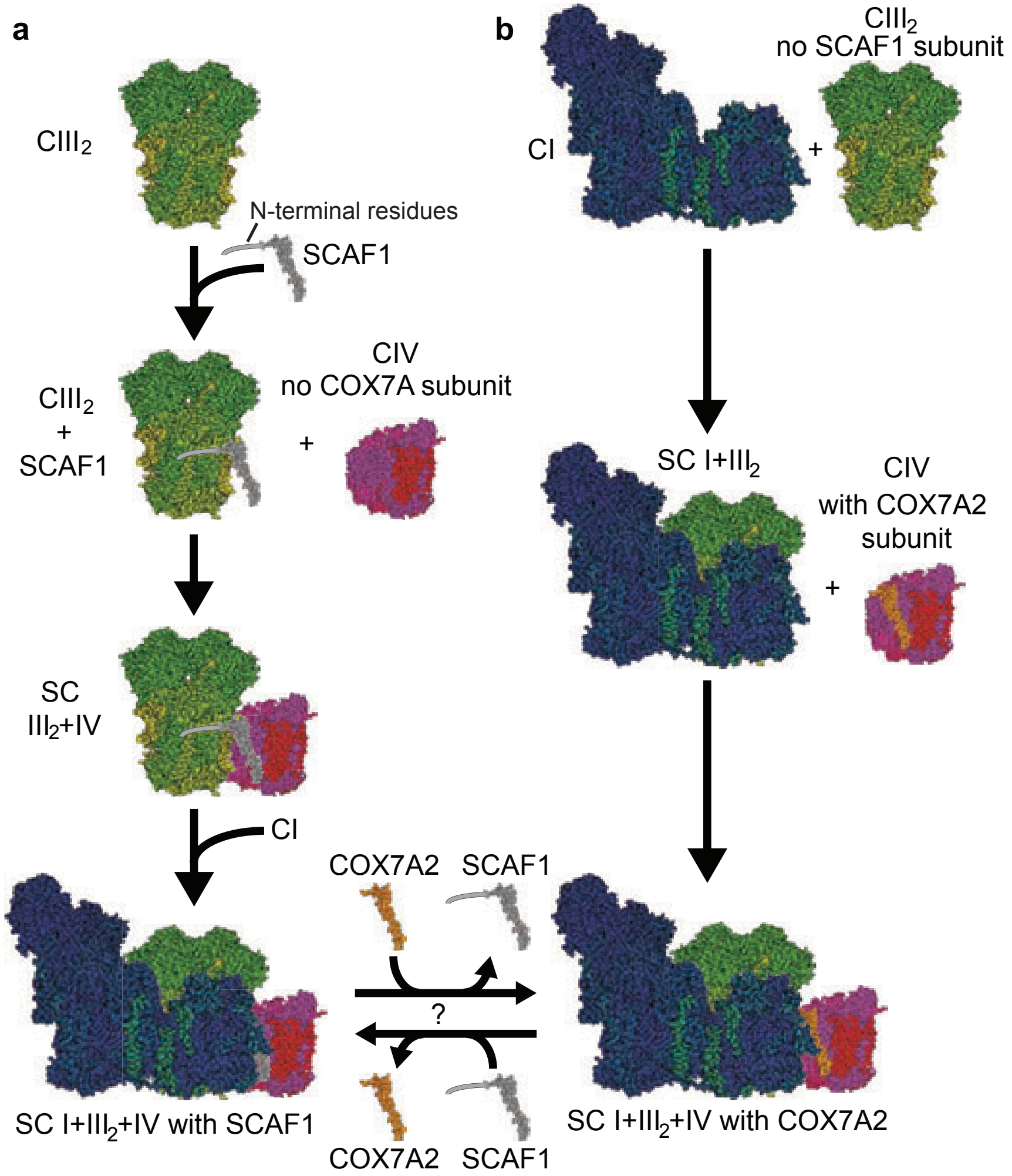
a
CIII2
N-terminal residues
SCAF1
CIII2
+
SCAF1
CIV
no COX7A subunit
+
SC
III2+IV
CI
SC I+III2+IV with SCAF1
b
CIII2
no SCAF1 subunit
CI
+
SC I+III2
CIV
with COX7A2
subunit
+
COX7A2
SCAF1
?
COX7A2
SCAF1
SC I+III2+IV with COX7A2

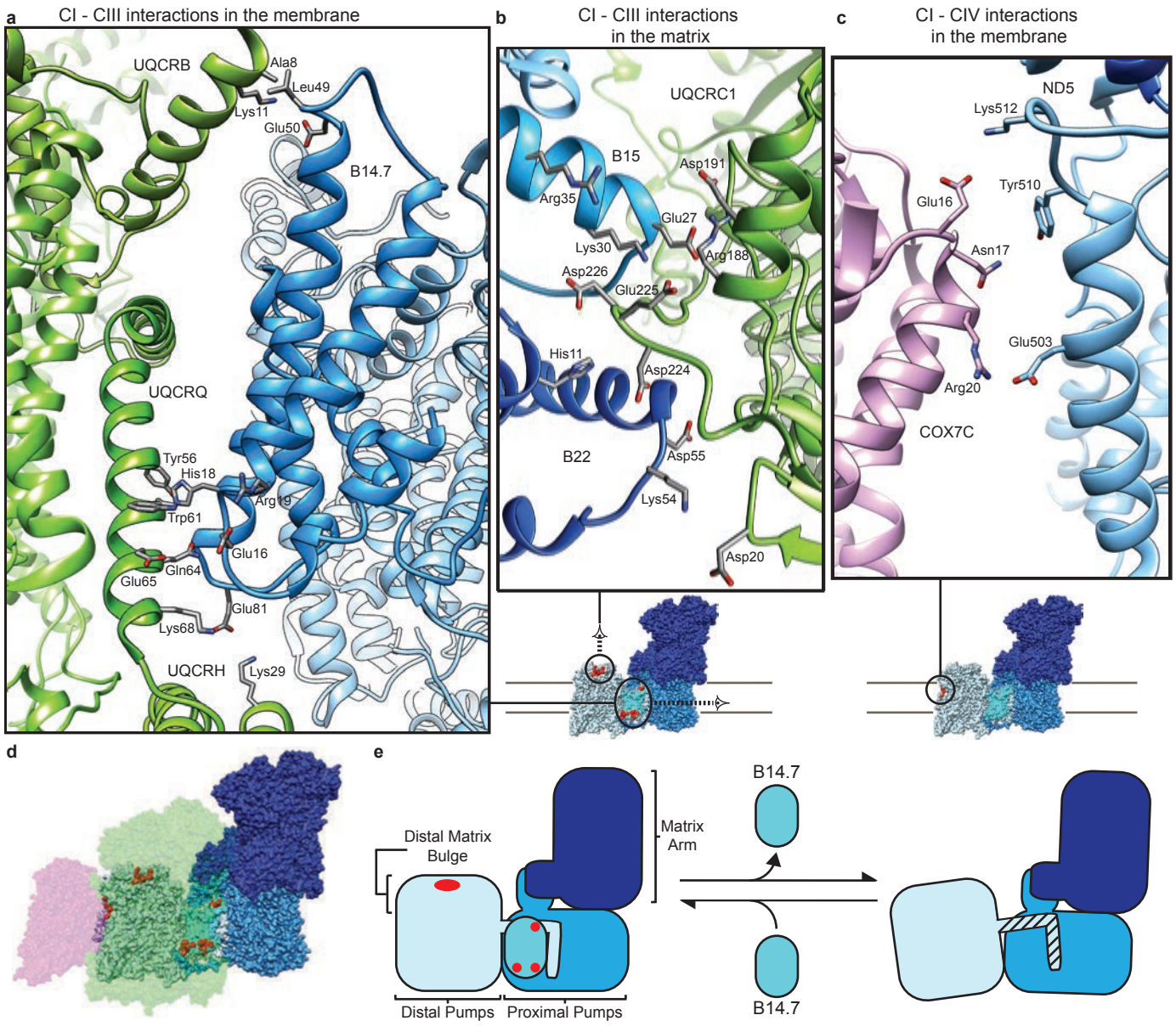
a
CI - CIII interactions in the membrane
UQCRB
Ala8
Leu49
Lys11
Glu50
B14.7
UQCRQ
Tyr56
His18
Arg19
Trp61
Glu16
Gln64
Glu65
Glu81
Lys68
UQCRH
Lys29
b
CI - CIII interactions
in the matrix
UQCRC1
B15
Asp191
Arg35
Glu27
Lys30
Arg188
Asp226
Glu225
His11
Asp224
B22
Asp55
Lys54
Asp20
c
CI - CIV interactions
in the membrane
ND5
Lys512
Tyr510
Glu16
Asn17
Glu503
Arg20
COX7C
d
e
Distal Matrix
Bulge
Matrix
Arm
B14.7
B14.7
Distal Pumps
Proximal Pumps

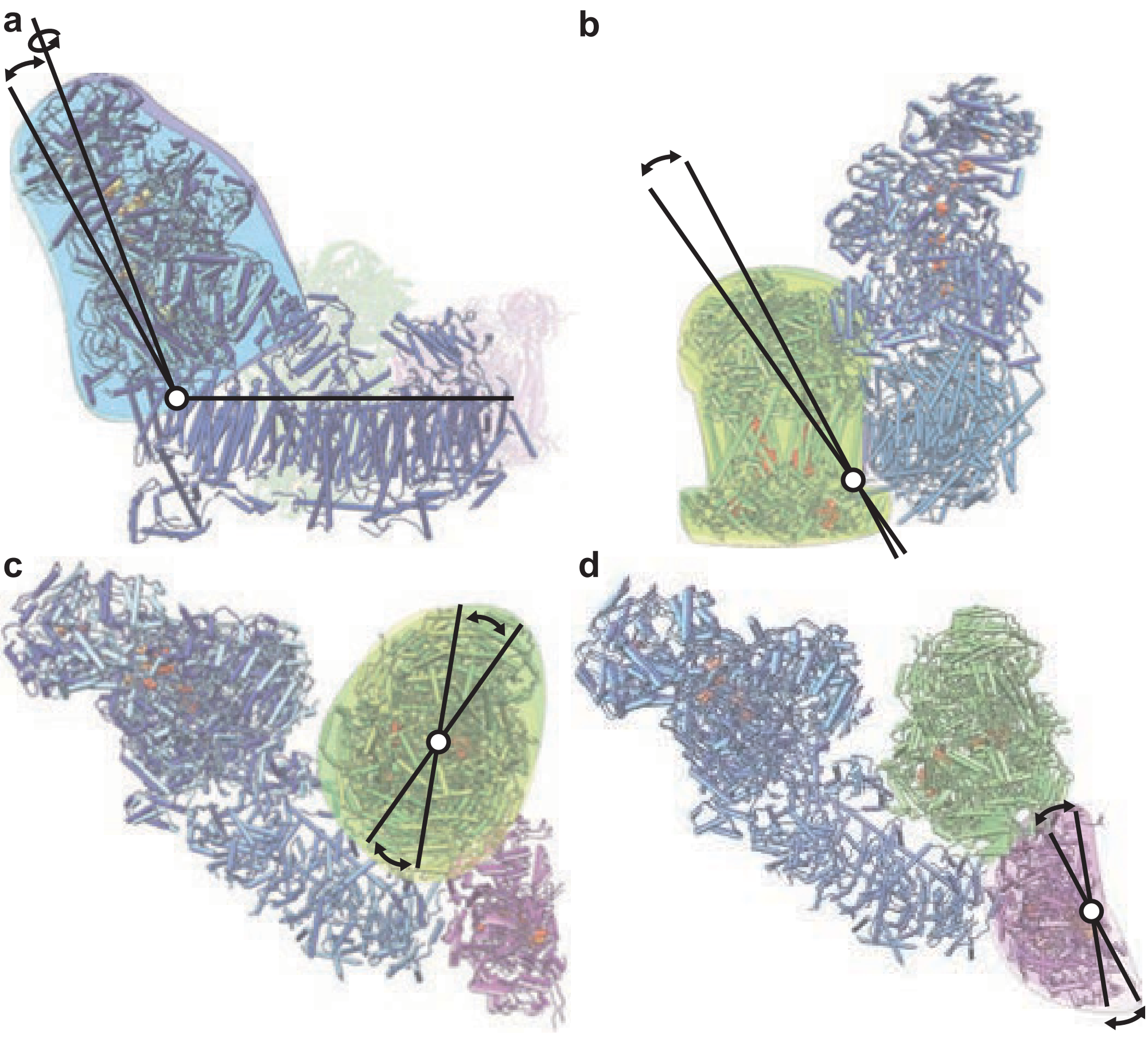
a
b
c
d

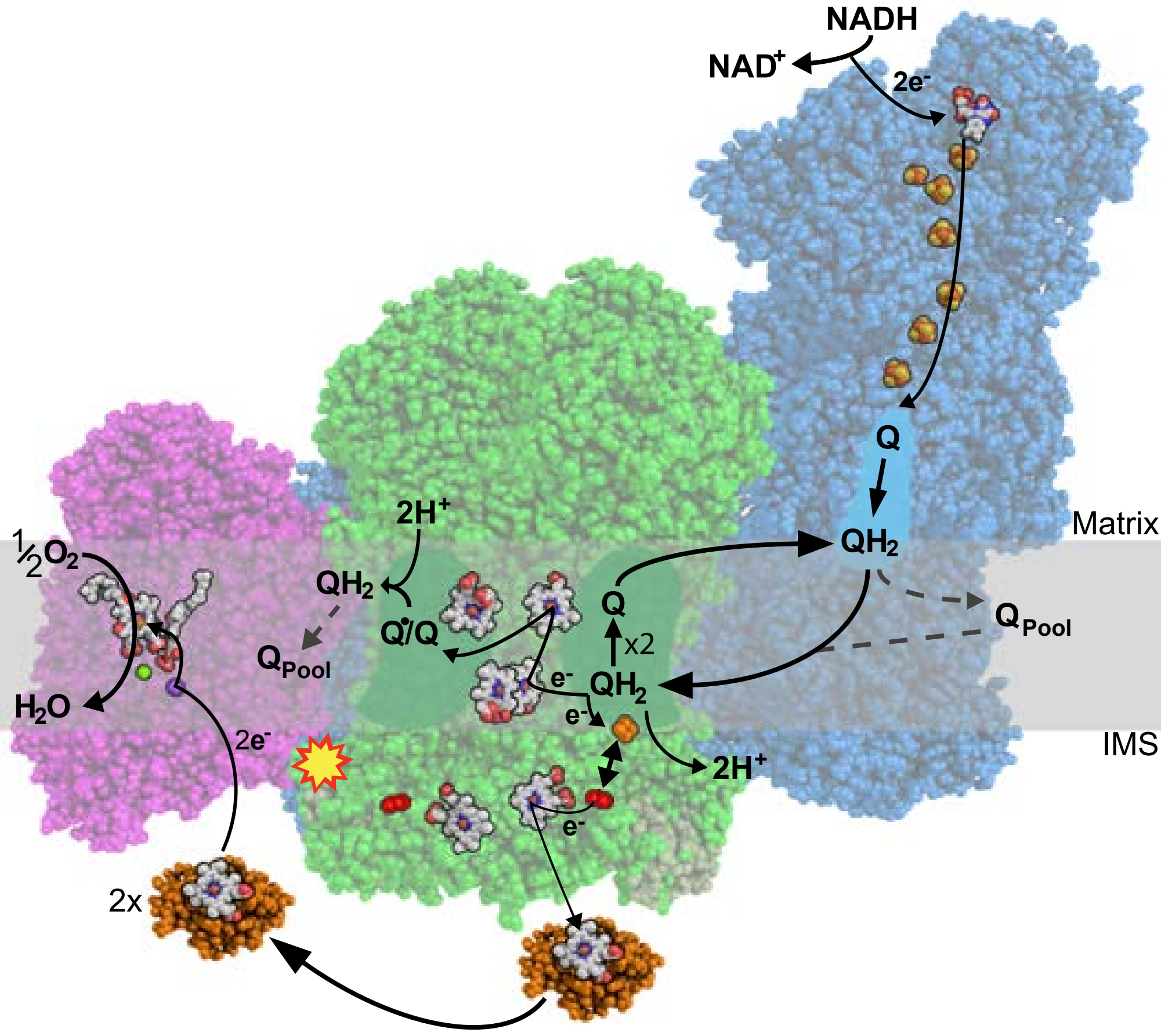
NADH
NAD+
2e-
Q
QH2
Matrix
2H+
½O2
QH2
Q•/Q
Q
QPool
x2
QPool
e-
QH2
e-
H2O
2e-
2H+
IMS
e-
2x